A Study on the Mechanism of the Proton Transport in Bacteriorhodopsin: The Importance of the Water Molecule

Katsumi Murata, Yasuyuki Fujii, Nobuyuki Enomoto, Masayuki Hata, Tyuji Hoshino, and Minoru Tsuda
Faculty of Pharmaceutical Sciences, Chiba University, Chiba 263-8522, Japan

ABSTRACT The mechanism of proton transport around the Schiff base in bacteriorhodopsin was investigated by ab initio molecular orbital (MO) calculations. Computations were performed for the case where there is a water molecule between the Schiff base and the Asp residue and for the case where there is no water molecule. Changes in the atomic configuration and potential energy through the proton transport process were compared between two cases. In the absence of water, the protonated Schiff base was not stable, and a proton was spontaneously detached from the Schiff base. On the other hand, a stable structure of the protonated Schiff base was obtained in the presence of water. This suggests that the presence of a water molecule is required for stability in the formation of a protonated Schiff base.

INTRODUCTION

Bacteriorhodopsin (Lanyi, 1993) is an integral membrane protein that was found in *Halobacterium salinarum*. It is known to have a seven-transmembrane helical structure (Henderson and Unwin, 1975) and to function as a light-driven proton pump. That is, light absorption in bacteriorhodopsin induces the transport of protons outside the cell, and the reaction cycle is completed within ~10 ms (Oesterhelt and Stoeckenius, 1973). Six intermediates, labeled J, K, L, M, N, and O, have been detected in the reaction cycle by spectroscopic studies (Lozier et al., 1975; Váró and Lanyi, 1991).

Recent developments in experimental techniques such as x-ray diffraction (Luecke et al., 1998) and Fourier transform infrared spectroscopy (Maeda et al., 1997) have made it possible to collect more detailed information on the proton transport mechanism during the photochemical reaction cycle. The seven transmembrane helices in bacteriorhodopsin make an internal cavity for the proton transport pathway and a binding pocket for a retinal chromophore. The retinal is bound to the ϵ-amino group of Lys^{216}, forming a protonated Schiff base structure. The retinal chromophore is a mixture of all-*trans* and 13-*cis*, 15-*anti* isomers in the dark. Only an all-*trans* bacteriorhodopsin contributes to proton transport in the reaction cycle induced by light absorption. Two important amino acid residues exist on both sides of the Schiff base: Asp^{96} on the cytoplasmic side and Asp^{85} on the extracellular side. These Asp residues have the ability to accept a proton, and they significantly contribute to the system for proton transport across the membrane via the Schiff base.

A photochemical reaction cycle of bacteriorhodopsin begins with light-induced isomerization of the retinal from the all-*trans* to the 13-*cis* configuration (Pettei et al., 1977; Braiman and Mathies, 1982), which produces the L state through the J and K intermediates. The proton of the Schiff base is transferred to Asp^{85} in the extracellular region (Subramaniam et al., 1992), producing an unprotonated state of the Schiff base (M state). Another proton is transferred to the Schiff base from Asp^{96} in the cytoplasmic region (Otto et al., 1989), which makes the Schiff base protonated again. This state is called the N state. Afterward, the retinal becomes an all-*trans* state in O and then returns to the initial state.

In this work we focused on two thermal steps in the proton transport cycle, the L-to-M and M-to-N processes, both of which are strongly related to the protonation of the Schiff base. To understand the proton transport mechanism around the Schiff base, the reaction was investigated using quantum chemical theoretical calculations. The results clarified that a water molecule existing between the Schiff base and the Asp residues has the role of maintaining a stable configuration of the protonated Schiff base and that the water molecule is indispensable for the reprotonation process of the Schiff base in the M-to-N conversion. The results also suggest that computations taking account of the dielectric constant in protein make possible a reasonable evaluation of the potential energy for the proton transport reaction.

METHODS

Modeling the reaction system

Construction of the model molecular system used in the present calculations was based on the three-dimensional atomic structure of bacteriorhodopsin (Protein Data Bank, entry code 2BRD) proposed by Grigorieff et al. (1996). To represent the atomic geometry involving the proton transport around the Schiff base, the retinal molecule and Lys^{216}, and Asp^{85} residues were extracted from the Grigorieff data. In the Grigorieff data, however, the retinal molecule has an all-*trans* conformation. Because the proton transfer reaction was known not to occur with the all-*trans* retinal, we converted the retinal molecule into the 13-*cis* conformation. Because of the limitation of the size of the model molecular system, some parts were simplified. Namely, C_{13} of the retinal was replaced by a methylene group,

Received for publication 5 April 1999 and in final form 28 April 2000.

Address reprint requests to Dr. Katsumi Murata, Faculty of Pharmaceutical Sciences, Chiba University, Chiba 263-8522, Japan. Tel.: +81-43-290-2926; Fax: +81-43-290-2925; E-mail: hoshi@p.chiba-u.ac.jp.

0006-3495/00/08/982/10 $2.00

and C_α of Asp^{85} and C_ϵ of Lys^{216} were replaced by methyl groups. This operation created the Asp residue $CH_3—COO^-$ and the Schiff base $CH_2{=}CH—CH{=}NH^+—CH_3$.

It has already been proposed that there is a water molecule between the Schiff base and the Asp residue (Cao et al., 1991; Maeda et al., 1994). In the present study, to clarify the role of this water molecule, we investigated differences in the model molecular system with and without the water molecule, as shown in Fig. 1. The two model systems represent the situation that the Schiff base is directly hydrogen-bonded to the Asp residue if the water molecule is not present (Fig. 1 *i*), whereas the Asp residue is connected to the Schiff base through a hydrogen-bonded water if the water molecule is present (Fig. 1 *ii*).

Computational procedure

Quantum chemical calculations were performed using a basis functional set, 6–31G**. The Schrödinger equations for the model molecular systems were solved by the Hartree-Fock (HF) method. The minimum points and the saddle point on the potential energy hypersurface were obtained by geometry optimization with the energy gradient method. Computation for frequency analysis was further performed for the structure of the saddle point, because the vibration of the molecular system in the transition state of the reaction must contain only one imaginary frequency. The steepest descent paths from the saddle point were calculated in both directions, following the normal vibrational mode of the imaginary frequency, which provided the lowest energy reaction path connecting a reactant and a product via the transition state. This reaction path is expressed in the mass-weighted intrinsic reaction coordinate (IRC).

To reproduce the environment inside the protein, computations were also performed, using the technique proposed by Onsager (1936). That is, the potential energy changes along the lowest energy reaction path were reestimated by taking into account the effect of the dielectric constant in the protein.

Because the electron correlation is not incorporated into the HF method, additional computations have been carried out, using the density functional theory (DFT). In the DFT calculations, the exchange energy was computed by the gradient-corrected formula developed by Becke (1993), and the correlation energy was computed with the formula developed by Lee et al. (1988). The computational program used was Gaussian 94 (Frisch et al., 1995).

RESULTS

Proton transport reaction without a water molecule

To find the atomic structures of the reactant and the product of the proton transport reaction, geometry optimizations were performed, using the model molecular system without a water molecule between the Schiff base and the Asp residue (Fig. 1 *i*). The atoms indicated by * in Fig. 1 are restricted to fixed positions during the calculations. Fig. 2 *A* shows the optimized structure, in which the Schiff base is unprotonated. The N atom of the Schiff base accepts a hydrogen bond from the O atom of the carboxyl side chain of the Asp residue. The stable structure was not obtained for the case where the Schiff base is protonated, which suggests that the Schiff base prefers to be unprotonated energetically. The structure in Fig. 2 *B* is obtained when the N-H distance is fixed at 1.00 Å. If no constraint in the N-H distance is applied, a proton is transferred to the Asp residue with a structural change from Fig. 2 *B* to Fig. 2 *A*, and the potential energy monotonically decreases by 24.0 kcal/mol.

Proton transport reaction with a water molecule

Geometry optimizations using the model molecular system shown in Fig. 1 *ii* revealed that the structures of the reactant and the product are stable in case where a water molecule is present. The atoms indicated by * were also fixed, and calculations were performed with the HF method. The optimized structures are shown in Fig. 3. Fig. 3 *C* shows the structure of the protonated state of the Schiff base, and Fig. 3 *D* shows the structure in the situation where a proton is transferred to the Asp residue. In Fig. 3, *C* and *D*, the N atom of the Schiff base accepts a hydrogen bond from the water molecule, which in turn accepts a hydrogen bond from the carboxyl side chain of the Asp residue.

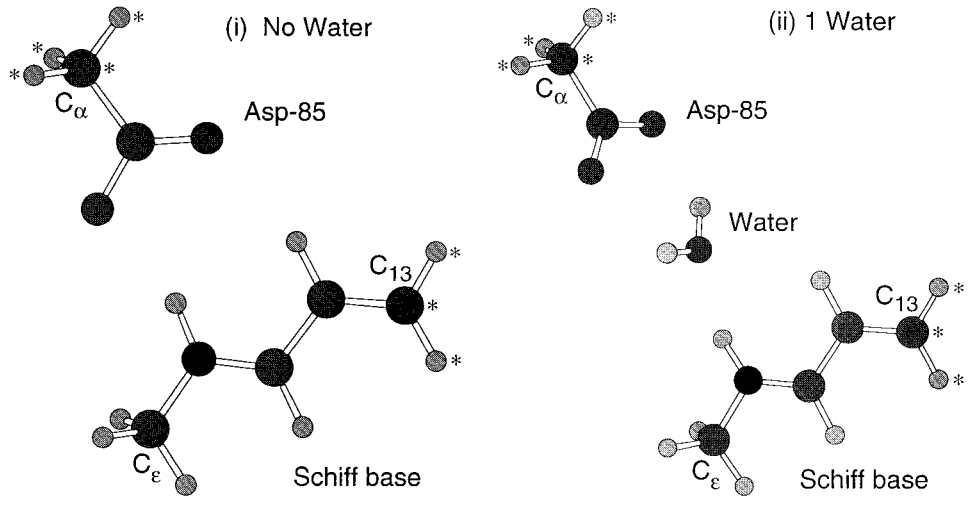

FIGURE 1 Model molecular systems for the case (*i*) where there is no water molecule between the Schiff base and Asp^{85} and for the case (*ii*) where a water molecule is present. The Schiff base and the Asp residue are represented by $CH_2{=}CH—CH{=}NH^+—CH_3$ and $CH_3—COO^-$, respectively. The atoms indicated by * are restricted to fixed positions during geometry optimization.

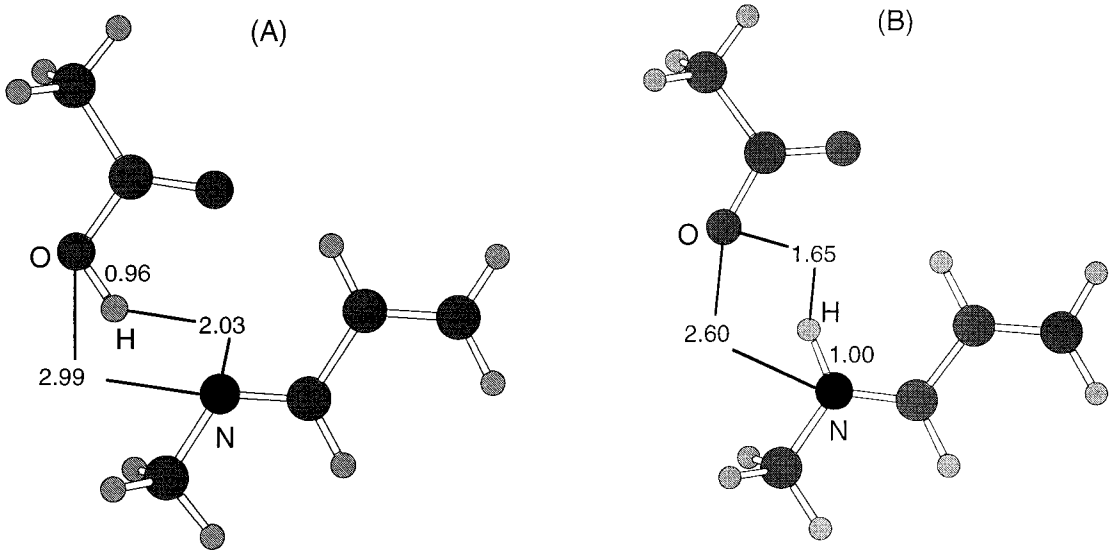

FIGURE 2 Optimized structures in the absence of a water molecule. (*A*) Structure of the unprotonated state. (*B*) Protonated state of the Schiff base under the constraint of a fixed N-H bond distance of 1.00 Å. The values represent the interatomic distances in Å.

A comparison of the potential energies of these two structures shows that the potential energy of the structure in Fig. 3 *C* is 33.6 kcal/mol higher than that in Fig. 3 *D*, which suggests that the unprotonated state of the Schiff base has an energetic advantage. The potential energy change from structure 3 *C* to structure 3 *D*, however, does not show a monotonic decrease. That is, there is a potential energy barrier to this reaction, which is a remarkable difference from the case in which a water molecule is not present. A geometry optimization, used to search for the saddle point, gave the structure of the transition state, as shown in Fig. 4 *E*. The results of frequency analysis indicated that this structure had only one vibrational mode corresponding to an imaginary frequency. The vibrational mode is shown by the arrows in Fig. 4 *E*.

Based on the results of frequency analysis, so-called IRC were performed for both the forward and reverse directions of the vibrational mode calculations to find the steepest

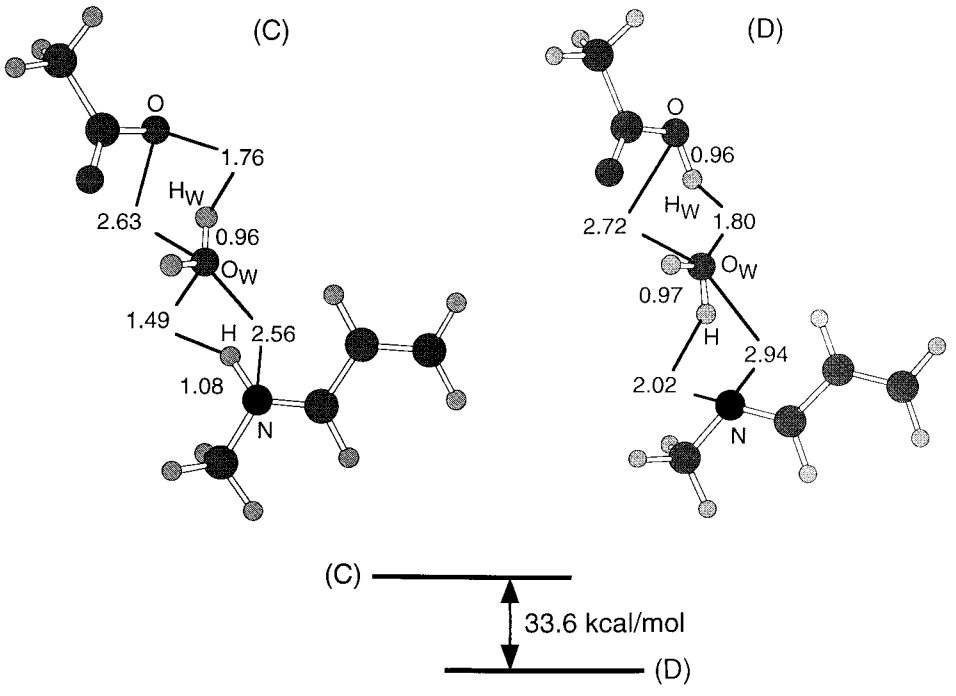

FIGURE 3 Optimized structures in the presence of a water molecule. (*C*) Structure of the protonated state of the Schiff base. (*D*) Structure of the unprotonated state. The values represent the interatomic distances in Å.

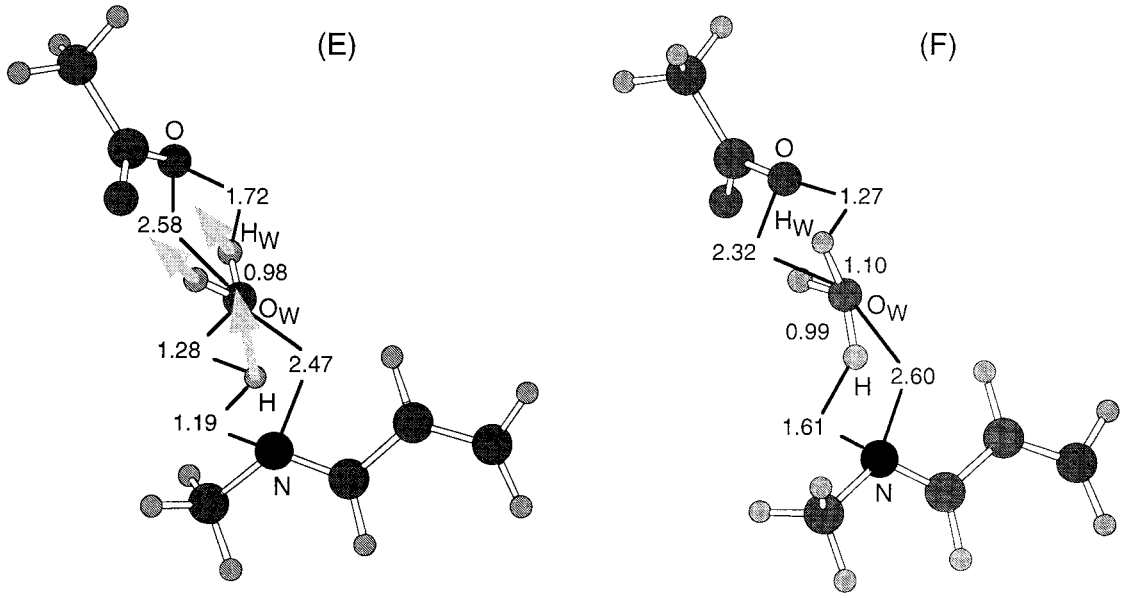

FIGURE 4 Optimized structure for the transition state (*E*) in the presence of a water molecule. Structure *F* corresponds to the inflection point in the potential energy curve of Fig. 5. The values represent the interatomic distances in Å. The vibrational mode corresponding to an imaginary frequency is indicated by arrows.

descent paths. The lowest energy reaction path connecting the reactant and the product was obtained (Fig. 5). Stable structures obtained by IRC calculations were confirmed to be identical to those in Fig. 3, *C* and *D*. The potential energy difference measured from the transition state is 0.5 kcal/mol for the protonated structure (Fig. 3 *C*) and 34.1 kcal/mol for the unprotonated structure (Fig. 3 *D*) in the HF level.

In the reaction path for deprotonation of the Schiff base, there appears to be an inflection point in its potential energy curve. The structure corresponding to this inflection point *F* is also shown in Fig. 4. In structure *F*, a proton released from the Schiff base approaches the O atom of the water molecule, resulting in the formation of a protonated water molecule, H_3O^+. With further progress of the deprotonation reaction, one of the H atoms is released from the water molecule and is transferred to the Asp residue to be bound to the O atom of the carboxyl side chain.

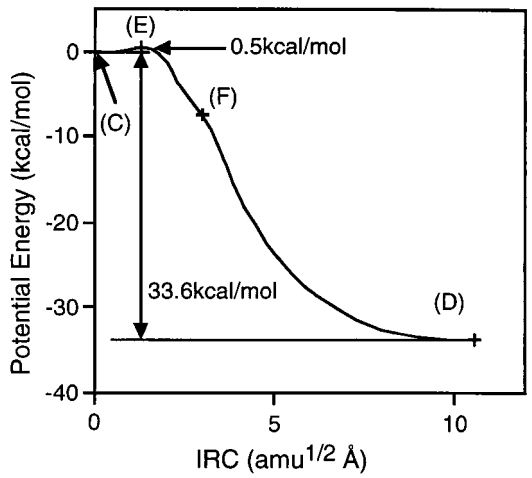

FIGURE 5 The potential energy curve along the lowest energy path for the proton transport reaction. The abscissa represents the intrinsic reaction coordinate (IRC), and the ordinate represents the potential energy. The activation energy for the deprotonation reaction is 0.5 kcal/mol, and the stabilization energy is 33.6 kcal/mol.

Effect of the dielectric constant in protein

For the purpose of improving the calculation by considering the environment inside the protein more exactly, the reaction path for the case where water is present was recalculated, taking into account the dielectric constant in protein. According to the Onsager reaction field method (Onsager, 1936), the model molecular system should be placed in a spherical cavity, with radius *a*, surrounded by a continuous medium of dielectric constant ϵ. In this work, the radius *a* was set at 4.51 Å, which was determined from the volume of the model molecular system. It has been reported that a dielectric constant of 20 is appropriate for the investigation a system that is surrounded by many ionized components in protein (Antosiewicz et al., 1996; Sham et al., 1998). Therefore, the dielectric constant ϵ was set at 20 in this study.

Calculations were performed in the same manner as the previous calculations. Geometry optimizations using the model molecular system of Fig. 1 *ii* with fixed atoms gave stable structures for the reactant and the product, as shown in Fig. 6. *C′* is the structure of the protonated state of the

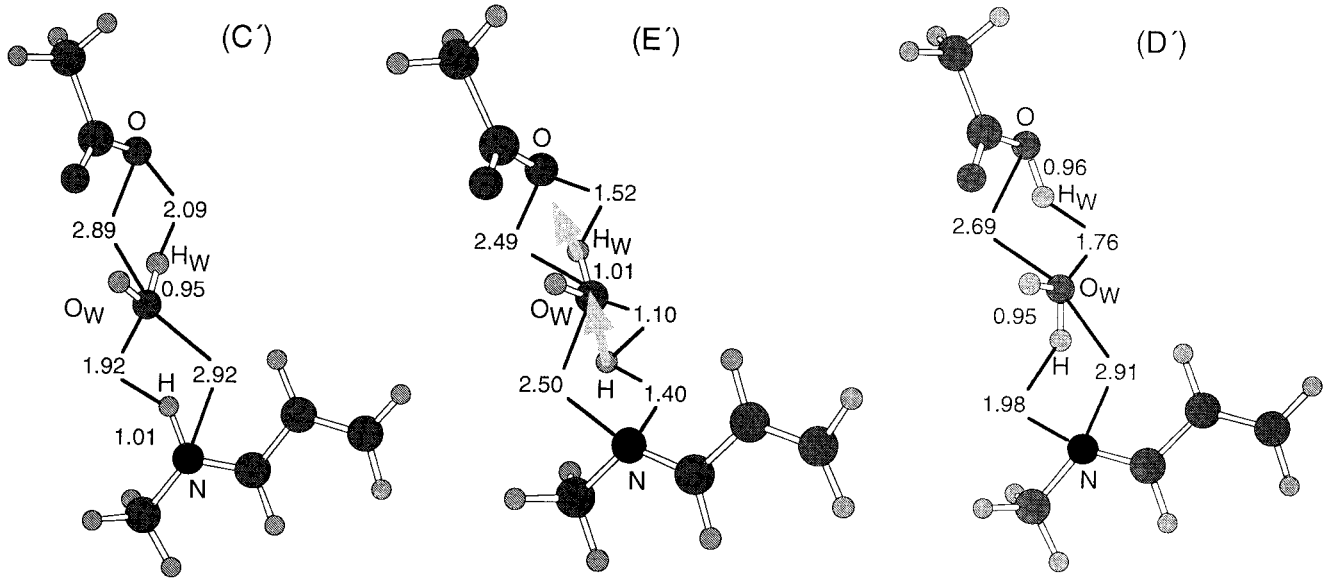

FIGURE 6 Optimized stable structures in the presence of a water molecule, obtained by taking into account the effect of the dielectric constant in protein. C' is the structure of the protonated state of the Schiff base, E' is the structure of the transition state, and D' is the structure of the unprotonated state. The vibrational mode corresponding to an imaginary frequency is indicated by arrows in E'.

Schiff base and D' is the structure of the deprotonated state. In both C' and D', the N atom of the Schiff base is connected to the O atom of the carboxyl side chain of the Asp residue through a hydrogen-bonded water. The potential energy of C' is 4.4 kcal/mol higher than that of D', which again suggests that the unprotonated state of the Schiff base has an energetic advantage. However, the energy difference between the protonated and unprotonated structures is small compared to the result obtained without considering the effect of the dielectric constant. The potential energy change from C' to D' is not a monotonic decrease but has an energy barrier. Hence geometry optimization was carried out to search for the saddle point. The optimized structure of the saddle point (E') is also shown in Fig. 6. The results of frequency analysis confirmed that this structure is appropriate for the transition state. The vibrational mode corresponding to an imaginary frequency is indicated by the arrows.

IRC calculations were performed for both directions of the reactant and the product to the vibrational mode, obtained by frequency analysis. Accordingly, the lowest energy reaction path was obtained (Fig. 7). The potential energy difference measured from the transition state is 16.9 kcal/mol for the protonated structure (C') and 21.3 kcal/mol for the deprotonated structure (D').

Effect of the inclusion of electron correlation

Computational results shown in Figs. 2–7 were obtained by the HF method. To check the influence of electron correlation, the proton transport process in bacteriorhodopsin has been recalculated by the DFT method with an Onsager reaction field ($\epsilon = 20$) for the case where water is present. Fig. 8 shows the optimized structure for the reactant (C''), the transition state (E''), and the product (D''). Atomic geometries of these structures determined by the DFT method appear to be consistent with those determined by the HF method. That is, C'' represents the protonated state of the Schiff base, and D'' is the unprotonated state. The structure E'' is also confirmed to be appropriate for the saddle point from the frequency analysis. The potential energy of the

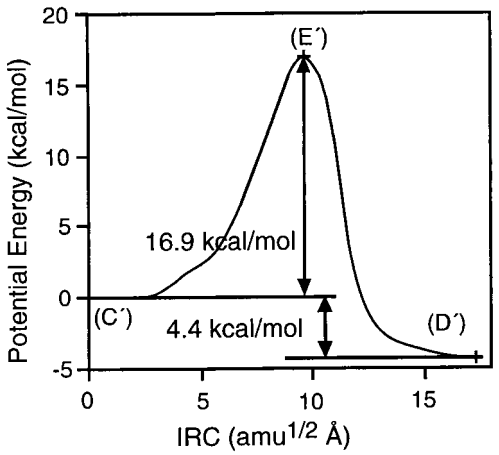

FIGURE 7 The potential energy curve along the lowest energy path for the proton transport reaction, obtained by taking into account the effect of the dielectric constant in protein. The abscissa represents the intrinsic reaction coordinate, and the ordinate represents the potential energy.

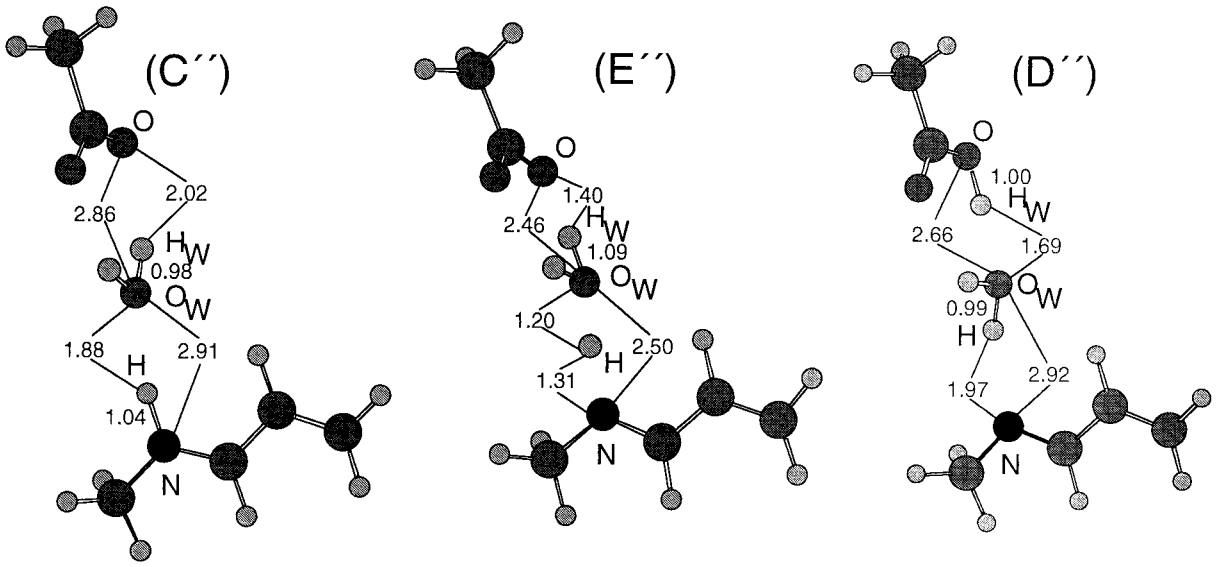

FIGURE 8 Optimized structures in the presence of water, calculated while taking into account the effects of the dielectric constant and the electron correlation. *C″*, *E″*, and *D″* correspond to the protonated, transition, and unprotonated states, respectively.

unprotonated structure (*D″*) is lower than that of the protonated structure (*C″*) by 5.7 kcal/mol, as seen in the potential energy curve of Fig. 9. The potential energy barrier is 3.9 kcal/mol measured from the protonated state and 9.6 kcal/mol from the unprotonated state.

Computations without geometrical restriction

Computations in the above subsections were performed under the restriction in which several atoms (indicated by * in Fig. 1) were fixed. Because proteins have some flexibility, it is interesting to examine the proton transport reaction when those fixed atoms change their positions slightly. The way in which the positions can be changed, however, has many variations, and no one set of fixed atom positions gives a perfect representation of the protein. Instead, computations without any constraint will give meaningful information, i.e., they provide an intrinsic reactivity between the Asp residue and the Schiff base. From this viewpoint, the proton transport reaction has been calculated by the DFT method with an Onsager reaction field ($\epsilon = 20$), without the restriction in Fig. 1 for the case where water is absent and the case where it is present.

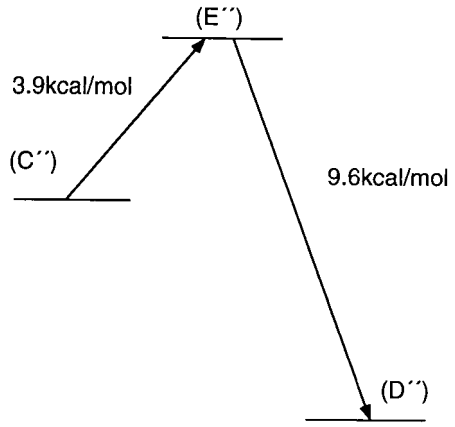

FIGURE 9 The potential energy change for the proton transport reaction shown in Fig. 8, obtained by taking into account of the effects of the dielectric constant and the electron correlation.

Fig. 10 *a* shows the optimized structure for the unprotonated state of the Schiff base in the absence of water, where the Asp residue is bound to the Schiff base through a hydrogen bond. The optimized structure is compatible with the result of Fig. 2, except for a slight decrease in the N-H distance. The stable structure was not obtained for the protonated state, and Fig. 10 *b* indicates the structure when the N-H distance is fixed to 1.09 Å.

The optimized structures for the protonated, transition, and unprotonated states in the presence of water are shown in Fig. 11, *c*, *e*, and *d*, respectively. Although the Asp residue changed the location and was not in the upright direction to the main chain of the Schiff base, the correlation among the Asp residue, the Schiff base, and the water molecule was maintained. The hydrogen atom bonded to the N atom of the Schiff base in protonated state *c* is transferred to the water molecule in the transition state *e*. Beyond the transition state, another hydrogen atom is transferred to the O atom of the Asp residue in *d*, which shows switching of the O-H connections around the water molecule.

A comparison of potential energy curves for the cases in which water is absent and water is present is presented in

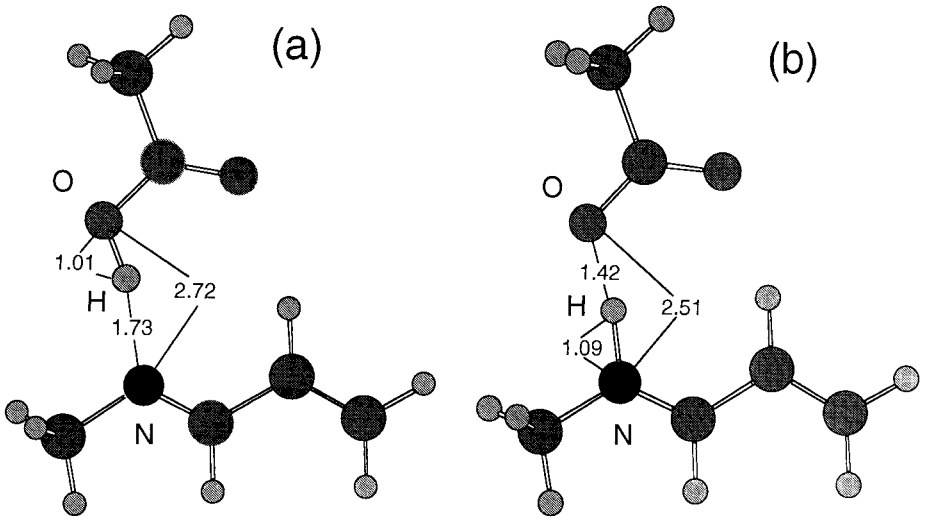

FIGURE 10 Optimized structures in the absence of water, obtained without geometric restriction. (*a*) Unprotonated state of the Schiff base. (*b*) Protonation under the constraint of a fixed N-H bond distance of 1.09 Å.

Fig. 12. In the absence of water, the energy monotonically decreases from *b* to *a*, which indicates the instability of the protonated state. On the other hand, there appears to be a potential energy barrier in the presence of water. The activation energy for the proton transport is calculated to be 1.8 kcal/mol, and the transport reaction gives an energetic stabilization of 8.4 kcal/mol. The reverse reaction requires an activation energy of 10.2 kcal/mol.

DISCUSSION

Role of the water molecule

In the case where there was no water molecule between the Schiff base and the Asp residue, the computational results suggested that no activation energy was required for the release of a proton from the Schiff base and that the structure of the protonated Schiff base was energetically unfavorable. That is, a transfer of the proton from the Schiff base takes place spontaneously. Therefore, generation of the N intermediate is unlikely to occur. On the other hand, it has been clarified from the energy curves in Figs. 5, 7, 9, and 12 that the structure of the protonated Schiff base is stable in the case where a water molecule is present. That is, the water molecule between the Schiff base and the Asp residue has the role of not only providing a hydrogen bond to form the proton transport pathway but also keeping the protonated Schiff base structure stable. Assuming that the Asp residue in the calculation is the proton donor Asp[96], the proton transport reaction corresponds to the M-to-N conversion in bacteriorhodopsin. Consequently, the presence of

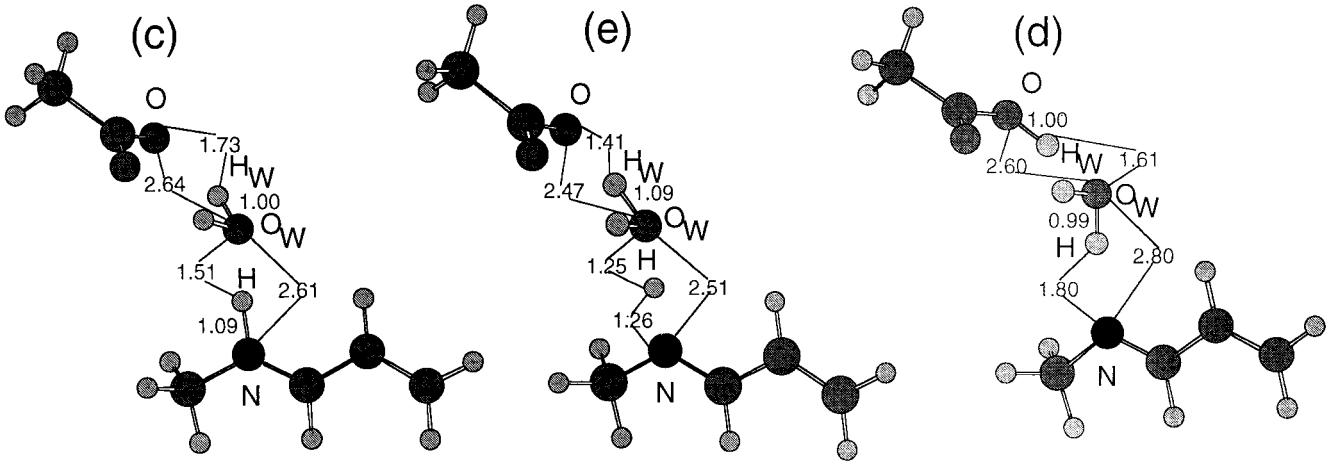

FIGURE 11 Optimized structures in the presence of water, obtained without geometric restriction. (*c*, *e*, and *d*) Protonated, transition, and unprotonated states, respectively.

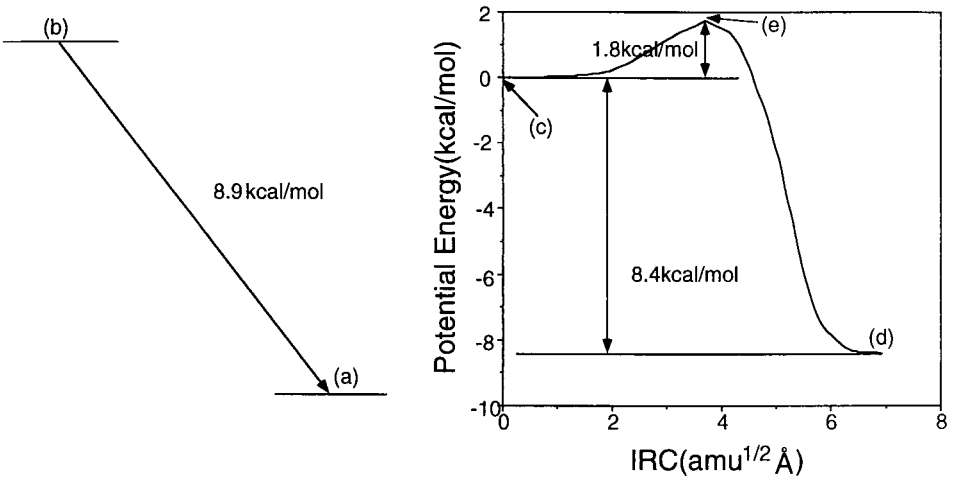

FIGURE 12 Potential energy changes for the proton transport reactions shown in Figs. 10 and 11. The potential energy curve for the case where water is present represents the lowest energy path in the intrinsic reaction coordinate (IRC).

a water molecule between the Schiff base and Asp[96] is concluded to be indispensable for the protonation of the Schiff base to generate the N intermediate structure.

In contrast, the conversion from the L to the M intermediate, the proton transfer to Asp[85], produces an unprotonated state of the Schiff base. Our results indicated that the unprotonated state is an energetically favorable structure in any case. Hence this conversion reaction would easily proceed, regardless of whether a water molecule is present. According to the experimental study by Cao et al. (1991), the addition of 58% sucrose to the sample reduced the concentration of water in the protein, which resulted in the blockage of the proton transport cycle specifically only for the M-to-N conversion. This is compatible with the present theoretical results.

Stability of the N intermediate with the protonated Schiff base

Our theoretical results clarified that the presence of a water molecule between the Schiff base and the Asp residue is important for keeping the protonated structure of the Schiff base stable in the N intermediate. Our results further suggest that the M intermediate, with an unprotonated structure, is more stable than the N intermediate. Experimental studies of the photochemical cycle in bacteriorhodopsin (Váró and Lanyi, 1991; Nagle, 1991) have shown that the free energy change due to proton transport between the Schiff base and the Asp residue is fairly small ($<$1.5 kcal/mol). The estimated energy change in the present study was 4.4–5.7 kcal/mol (in Figs. 7 and 9), taking into account the effect of the dielectric constant in protein, with fixed atoms for geometry restriction. Despite the small difference between the experimental value and the present theoretical result, the present computations seems to provide a reasonable evaluation of the potential energy during the proton transport reaction.

Reprotonation of the Schiff base in the proton transport cycle

It was revealed from our study that an unprotonated state of the Schiff base is energetically more stable than a protonated state. This means that the generation of the N intermediate from the M intermediate is unfavorable because of the disadvantage of the protonation of the Schiff base. Nevertheless, bacteriorhodopsin effectively functions as a proton pump to achieve proton transport to the extracellular side. That is, reprotonation of the Schiff base is very important for the mechanism of bacteriorhodopsin.

In regard to the above question, Fodor et al. (1988) proposed a "C-T model" that invoked isomerization-driven protein conformational change. The conformational change was supposed to work like a switch for the reprotonation. Furthermore, Brown et al. (1995) detected a conformational change in helix F, which is one of the seven transmembrane helices, after a proton was transferred from the Schiff base to the proton acceptor Asp[85] in the L-to-M conversion. It seems reasonable to assume that such a conformational change of a protein induces transformation of the local structure around the reaction active site and promotes reprotonation of the Schiff base. This point will be our next target of investigation in the future.

Evaluation of the dielectric constant in protein

It is known that the dielectric constant in protein does not have the same value throughout the protein but varies depending on the environment at a local spot in the protein (Laberge, 1998). For example, the dielectric constant is low (2–4) in an area where ionized components are sparsely distributed in protein. On the other hand, the dielectric constant is high in an area where many ionized components exist. According to Antosiewicz et al. (1996), the value of pKa for ionized groups in protein was correctly estimated in

the case where the dielectric constant was 20, whereas the estimation was largely deviated in the case where the dielectric constant was 4. Furthermore, Sham et al. (1998) proposed that evaluation of the interaction of electric charges in protein should be carried out with the dielectric constant set to a value much higher than 4. Hence it would be important to assess the effect of the dielectric constant on the computational results. Our present computations have revealed that there are stable structures for both the protonated and unprotonated states of the Schiff base in the presence of water. Then the potential energy differences were reevaluated, using several different values for the dielectric constant. Computations for the optimization of the protonated and unprotonated states were routinely carried out with the values $\epsilon = 1$, 4, 20, and 40, using the restricted model in Fig. 1 *ii*. The potential energy difference between the protonated and unprotonated states is shown in Fig. 13 as a function of dielectric constant, where the energy of the unprotonated state is always lower than that of the protonated state. It is noteworthy that the potential energy difference gradually decreases with an increasing dielectric constant. According to an experimental report (Váró and Lanyi, 1991; Nagle, 1991), the energy change during the protein transport in bacteriorhodopsin is fairly small (~1.5 kcal/mol). Hence computations are compatible with the experiments when the dielectric constant is over 20. In this work we also used the DFT method for the inclusion of electron correlation. Fig. 13 further shows a energy comparison in the DFT calculation (*dashed line*). The deviation of the potential energies between the HF and DFT methods is small, except for the case where $\epsilon = 1$.

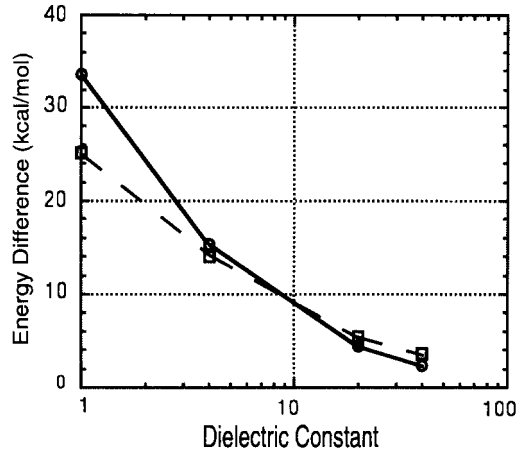

FIGURE 13 Potential energy difference between the protonated and unprotonated states of the Schiff base, computed for the case where water is present. The energy difference (protonated versus unprotonated state) is presented as a function of the dielectric constant. The solid and dashed lines denote the results of the HF and the DFT methods, respectively.

CONCLUSIONS

Quantum chemical calculations provided the following findings on the reaction mechanism of proton transport in bacteriorhodopsin: 1) Concerning the conversion from the L to the M intermediate, deprotonation of the Schiff base easily occurs regardless of whether there is a water molecule between the Schiff base and Asp^{85}. 2) The water molecule between the Schiff base and Asp^{96} has the role of maintaining the Schiff base in a stable protonated state. This water molecule is indispensable for the reprotonation of the Schiff base in the conversion process from the M to the N intermediate.

REFERENCES

Antosiewicz, J., J. A. McCammon, and M. K. Gilson. 1996. The determinants of pK_as in proteins. *Biochemistry.* 35:7819–7833.

Becke, A. D. 1993. Density-functional thermochemistry. III. The role of exact exchange. *J. Chem. Phys.* 98:5648–5652.

Braiman, M., and R. Mathies. 1982. Resonance Raman spectra of bacteriorhodopsin's primary photoproduct: evidence for a distorted 13-*cis* retinal chromophore. *Proc. Natl. Acad. Sci. USA.* 79:403–407.

Brown, L. S., G. Váró, R. Needleman, and J. K. Lanyi. 1995. Functional significance of a protein conformation change at the cytoplasmic end of helix F during the bacteriorhodopsin photocycle. *Biophys. J.* 69: 2103–2111.

Cao, Y., G. Váró, M. Chang, B. Ni, R. Needleman, and J. K. Lanyi. 1991. Water is required for proton transfer from aspartate-96 to the bacteriorhodopsin Schiff base. *Biochemistry.* 30:10972–10979.

Fodor, S. P. A., J. B. Ames, K. Gebhard, E. M. M. van den Berg, W. Stoeckenius, J. Lugtenburg, and R. A. Mathies. 1988. Chromophore structure in bacteriorhodopsin's N intermediate: implications for the proton-pumping mechanism. *Biochemistry.* 27:7097–7101.

Frisch, M. J., G. W. Trucks, H. B. Schlegel, P. M. W. Gill, B. G. Johnson, M. A. Robb, J. R. Cheeseman, T. Keith, G. A. Petersson, J. A. Montgomery, K. Raghavachari, M. A. Al-Laham, V. G. Zakrzewski, J. V. Ortiz, J. B. Foresman, J. Cioslowski, B. B. Stefanov, A. Nanayakkara, M. Challacombe, C. Y. Peng, P. Y. Ayala, W. Chen, M. W. Wong, J. L. Andres, E. S. Replogle, R. Gomperts, R. L. Martin, D. J. Fox, J. S. Binkley, D. J. Defrees, J. Baker, J. P. Stewart, M. Head-Gordon, C. Gonzalez, and J. A. Pople. 1995. Gaussian 94, Revision E.2. Gaussian, Inc., Pittsburgh, PA.

Grigorieff, N., T. A. Ceska, K. H. Downing, J. M. Baldwin, and R. Henderson. 1996. Electron-crystallographic refinement of the structure of bacteriorhodopsin. *J. Mol. Biol.* 259:393–421.

Henderson, R., and P. N. T. Unwin. 1975. Three-dimensional model of purple membrane obtained by electron microscopy. *Nature.* 257:28–32.

Laberge, M. 1998. Intrinsic protein electric fields: basic non-covalent interactions and relationship to protein-induced Stark effects. *Biochim. Biophys. Acta.* 1386:305–330.

Lanyi, J. K. 1993. Proton translocation mechanism and energetics in the light-driven pump bacteriorhodopsin. *Biochim. Biophys. Acta.* 1183: 241–261.

Lee, C., W. Yang, and R. G. Parr. 1988. Development of the Colle-Salvetti correlation-energy formula into a functional of the electric density. *Phys. Rev. B.* 37:785–789.

Lozier, R. H., R. A. Bogomolni, and W. Stoeckenius. 1975. Bacteriorhodopsin: a light-driven proton pump in *Halobacterium halobium*. *Biophys. J.* 15:955–962.

Luecke, H., H.-T. Richter, and J. K. Lanyi. 1998. Proton transfer pathways in bacteriorhodopsin at 2.3 Ångstrom resolution. *Science.* 280: 1934–1937.

Maeda, A., H. Kandori, Y. Yamazaki, S. Nishimura, S. Hatanaka, Y.-S. Chon, J. Sasaki, R. Needleman, and J. K. Lanyi. 1997. Intermembrane

signaling mediated by hydrogen-bonding of water and carboxyl groups in bacteriorhodopsin and rhodopsin. *J. Biochem.* 121:399–406.

Maeda, A., J. Sasaki, Y. Yamazaki, R. Needleman, and J. K. Lanyi. 1994. Interaction of aspartate-85 with a water molecule and the protonated Schiff base in the L intermediate of bacteriorhodopsin: a Fourier transform infrared spectroscopic study. *Biochemistry.* 33:1713–1717.

Nagle, J. F. 1991. Photocycle kinetics: analysis of Raman data from bacteriorhodopsin. *Photochem. Photobiol.* 54:897–903.

Oesterhelt, D., and W. Stoeckenius. 1973. Functions of a new photoreceptor membrane. *Proc. Natl. Acad. Sci. USA.* 70:2853–2857.

Onsager, L. 1936. Electric moments of molecules in liquids. *J. Am. Chem. Soc.* 58:1486–1493.

Otto, H., T. Marti, M. Holz, T. Mogi, M. Lindau, H. G. Khorana, and M. P. Heyn. 1989. Aspartic acid-96 is the internal proton donor in the reprotonation of the Schiff base of bacteriorhodopsin. *Proc. Natl. Acad. Sci. USA.* 86:9228–9232.

Pettei, M. J., A. P. Yudd, K. Nakanishi, R. Henselman, and W. Stoeckenius. 1977. Identification of retinal isomers isolated from bacteriorhodopsin. *Biochemistry.* 16:1955–1959.

Sham, Y. Y., I. Muegge, and A. Warshel. 1998. The effect of protein relaxation on charge-charge interactions and dielectric constants of proteins. *Biophys. J.* 74:1744–1753.

Subramaniam, S., D. A. Greenhalgh, and H. G. Khorana. 1992. Aspartic acid 85 in bacteriorhodopsin functions both as proton acceptor and negative counterion to the Schiff base. *J. Biol. Chem.* 267:25730–25733.

Váró, G., and J. K. Lanyi. 1991. Thermodynamics and energy coupling in the bacteriorhodopsin photocycle. *Biochemistry.* 30:5016–5022.